ISTITUTO NAZIONALE DI FISICA NUCLEARE
Laboratori Nazionali di Frascati

LNF-85/64

G.Bologna et al.: PRIMARY COSMIC-RAY SPECTRUM AT ENERGIES $\sim(10^{13}-10^{16})$ eV FROM MULTIPLE MUON EVENTS IN NUSEX EXPERIMENT

Estratto da:
Nuovo Cimento 8C, 76 (1985)

Servizio Documentazione
dei Laboratori Nazionali di Frascati
Cas. Postale 13 - Frascati (Roma)

IL NUOVO CIMENTO Vol. 8 C, N. 1 Gennaio-Febbraio 1985

Primary Cosmic-Ray Spectrum at Energies $\sim(10^{13}\div10^{16})$ eV from Multiple Muon Events in NUSEX Experiment.

G. Bologna, C. Castagnoli, A. Castellina, A. Ciocio
B. D'Ettorre Piazzoli, P. Galeotti, G. Mannocchi, P. Picchi
O. Saavedra and S. Vernetto

Istituto di Fisica Generale - Torino, Italia
Istituto di Cosmogeofisica del C.N.R. - Torino, Italia

E. Bellotti, E. Fiorini, C. Liguori, P. Negri, A. Pullia, S. Ragazzi
M. Rollier and L. Zanotti

Dipartimento di Fisica dell'Università - Milano, Italia
Istituto Nazionale di Fisica Nucleare - Sezione di Milano, Italia

G. Battistoni, C. Bloise, P. Campana, V. Chiarella, E. Iarocci
G. P. Murtas, G. Nicoletti and L. Satta

Istituto Nazionale di Fisica Nucleare - Laboratori Nazionali di Frascati, Italia

D. C. Cundy and M. Price

C.E.R.N., European Organization for Nuclear Reserach - Geneva, Switzerland

(ricevuto il 16 Ottobre 1984)

Summary. — The multiple-muon rates measured in the NUSEX experiment at a vertical depth of 5000 hg/cm² s.r. are compared with some current models of the primary cosmic-ray composition. Monte Carlo simulations as well as analytical formulae which take into account the geometrical and acceptance features of the apparatus have been used in calculations. A good agreement is found with a model in which the relative fraction of primary heavy nuclei does not increase significantly up to about 10^{16} eV. This model reproduces very well both the all-nucleon flux measured in the range $(10^{13}\div10^{14})$ eV and the all-particle spectrum up to 10^{16} eV.

PACS. 94.40. – Cosmic rays.

1. – Introduction.

Direct observations of primary cosmic rays have been carried out with experiments on balloons or satellites up to about $5 \cdot 10^{14}$ eV. Above this energy the flux is so low that information on the primary spectrum and its composition come in an indirect way from the analysis of extensive air showers ([1]), from energetic photon-hadron families (A-jets) at mountain altitudes ([2]), measurements of hadron spectra in the atmosphere ([3]) and observations of parallel muon groups (muon bundle) ([4]). However, these studies have given conflicting results for the primary composition. The interpretation of many measurements has led to the conclusion that the relative composition of various nuclear groups changes with increasing energy, the primary flux at energies $(10^{15} \div 10^{16})$ eV being strongly dominated by heavy primaries ([1a]). On the other hand, a recent analysis ([5]) evidences that cosmic-ray shower propagation has to be interpreted in terms of changes in the nature of high-energy hadronic interactions. Differences in the details of interaction models, assumptions on primary composition as well as different approaches in air shower Monte Carlo simulation are the main causes of these different interpretations. Moreover, many of

---

([1]) *a*) G. B. YODH: *Composition of Cosmic Rays at High Energies*, in *Proceedings of the XVI Rencontre de Moriond, Astrophysics Meeting, Les Arcs, France* (1981), p. 23. *b*) G. B. YODH, J. A. GOODMAN, S. C. TONWAR and R. W. ELLSWORTH: *Phys. Rev. D.* **29**, 892 (1984); *c*) G. THORNTON and R. CLAY: *Phys. Rev. Lett.*, **45**, 1463 (1982); *d*) A. A. ANDAM, M. P. CHANTLER, M. A. B. CRAIG, T. J. L. MCCOMB, K. J. ORFORD, K. E. TURVER and G. M. WALLEY: *Phys. Rev. D*, **26**, 23 (1982); *e*) J. A. GODMAN, R. W. ELLSWORTH, A. S. ITO, J. R. MCFALL, F. SIOHAN, R. E. STREITMATTER, S. C. TONWAR, P. R. VISWANATH and G. B. YODH: *Phys. Rev. D*, **26**, 1043 (1982).

([2]) *a*) C. M. G. LATTES, Y. FUJIMOTO and S. HASEGAWA: *Phys. Rep.*, **65**, 153 (1980). *b*) M. AMENOMORI, E. KONISHI, H. NANJO, K. MIZUTANI, K. KASAHARA, S. TORII, T. YUDA, T. SHIRAI, N. TATEYAMA, T. TAIRA, I. MITO, M. SHIBATA, H. SUGIMOTO, K. TAIRA and N. HOTTA: *Phys. Rev. D*, **25**, 2807 (1982). *c*) M. AKASHI, M. AMENOMORI, E. KONISHI, H. NANJO, Z. WATANABE, K. MIZUTANI, K. KASAHARA, S. TORII, T. YUDA, T. SHIRAI, N. TATEYAMA, T. TAIRA, I. MITO, M. SHIBATA, H. SUGIMOTO, K. TAIRA and N. HOTTA: *Phys. Rev. D*, **24**, 2353 (1981).

([3]) *a*) S. I. NIKOLSKI: *Izv. Acad. Sci. USSR*, **34**, 1849 (1970). *b*) M. AKASHI, M. AMENOMORI, E. KONISHI, H. NANJO, Z. WATANABE, M. ICHIJU, K. MIZUTANI, K. KASAHARA, S. TORII, T. YUDA, T. SHIRAI, N. TATEYANA, T. TAIRA, I. MITO, M. SHIBATA, H. SUGIMOTO, K. TAIRA and N. HOTTA: *Nuovo Cimento A*, **65**, 355 (1981).

([4]) *a*) For a recent analysis of Homestake and Utah results, see J. W. ELBERT, T. K. GAISSER and T. STANEV: *Phys. Rev. D*, **27**, 1448 (1983). *b*) L. BERGAMASCO, H. BILOKON, C. CASTAGNOLI, B. D'ETTORRE PIAZZOLI, G. MANNOCCHI and P. PICCHI: *Lett. Nuovo Cimento*, **26**, 609 (1979). *c*) L. BERGAMASCO, B. D'ETTORRE PIAZZOLI and G. MANNOCCHI: *Lett. Nuovo Cimento*, **27**, 71 (1980). *d*) T. K. GAISSER and T. STANEV: talk presented at the *XVIII International Cosmic Ray Conference* (Bangalore, 1983).

([5]) J. KEMPA and J. WDOWCZYK: *J. Phys. G*, **9**, 1271 (1983).

these calculations do not include in an adequate way a realistic simulation of the experimental conditions. For these reasons it is difficult to reach firm conclusions about primary composition above 10^{14} eV, the knowledge of which is important in understanding the origin and propagation of cosmic rays in the Galaxy.

In this respect, studies of the frequency distribution of high-energy (> 1 TeV) muon bundles of different multiplicities appear as the best way to disentangle the competing astrophysics and particle physics effects. In fact, due to the lack of interactions of muons with air nuclei, the muon component at very high energy contains the cleanest information on the feature of the primary cosmic-ray first interactions. Moreover, a procedure to take into account the geometrical features of the apparatus has been developed ([6]), along with a general formula to calculate absolute muon bundles rates in which the cosmic-ray spectrum and interaction properties appear separately. By fixing the high-energy physics model one can study the dependence of the multiple-muon frequency on the nature of primaries.

We present here the results from the analysis of the multiple-muon events recorded by the NUSEX detector in the Mt. Blanc Laboratory over a running time of 17854.4 hours. We use the results of a Monte Carlo simulation of atmospheric showers and muon propagation in rock first developed by ELBERT ([7]), and adapted to our experimental site by GAISSER and STANEV ([8]). Then compare the experimental multiple-muon rates to the calculated ones in terms of trials primary cosmic-ray spectra. We make plausible assumptions about the shape of the spectra for protons and lighter nuclei and consider the exponent of heavy-nuclei spectrum as a free parameter to be determined by the requirement of best agreement between the experimental and calculated rates. The reason for this approach is to check the most popular idea that the nuclear composition varies with increasing energy, leading to the dominance of heavier nuclei at energies ($10^{15} \div 10^{16}$) eV.

2. – The apparatus.

The nucleon stability experiment (NUSEX) has been in operation since May 1982 in the Mont Blanc Laboratory of the I.C.G.F. (CNR), garage 17th, inside the tunnel linking Italy and France at a vertical depth of 5000 hg/cm^2 s.r.

([6]) G. BOLOGNA, A. CASTELLINA, B. D'ETTORRE PIAZZOLI, G. MANNOCCHI, P. PICCHI and S. VERNETTO: to be published in *Nucl. Instrum. Methods.*

([7]) *a*) J. W. ELBERT: *Proceedings of the DUMAND Workshop*, edited by A. ROBERTS, Vol. **2** (La Jolla, Cal., 1978), p. 101. *b*) J. W. ELBERT and T. K. GAISSER: *Proceedings of the XVI International Cosmic Ray Conference*, Vol. **8** (Kyoto, 1979), p. 42.

([8]) T. K. GAISSER and T. STANEV: private communication.

The detector consists of a cube (each side = 3.5 m) made of 136 horizontal iron plates, 1 cm thick, interleaved with planes of plastic streamer tubes (total number of tubes: 42 880). Each layer (iron + device) is 2.7 cm thick, with mean density $\varrho = 3.5$ g/cm^3. The basic element of our tubes is a comb profile (3.5 m long) of extructed PVC, which consists of eight open cells (cross-section (9×9) mm^2) coated with graphite (resistivity $\geqslant 5 \cdot 10^4$ Ω/square). Three sides of the tube cathode are made by the profile, the fourth by a PVC cover which is also coated. The wire diameter is 100 μm, and it is kept centred by PVC spacers every half a meter. A PVC container houses two profiles, and on the exterior there are only the connector for the gas and the HV supply. The limited streamer ([9,10]) is a self-triggered and saturated mode localized in a few millimetres. It allows the use of thick sense wires and is characterized by a large signal (~ 1 mA peak current), and exhibits noiseless operation in a wide HV range.

In fact the read-out is not through the wires but through the x and y strips which pick-up the pulses induced outside the cathode. This bidimensional read-out makes it possible to record the detailed spatial pattern. The electronic chain to process the strip signal (triangular shape, pulse height $\geqslant 4$ mV/50 Ω and width ~ 40 ns) is very simple: an amplifier, a comparator with variable threshold, a one-shot, and a shift register bit. The electronic cards on the end of the x and y strips of the same plane are interconnected by a bus. The bus cables provide the read-out control signals and the data path to the processor. An OR signal for each plane, from the y strip, is used for trigger purpose.

The loosest trigger that we take is the « AND » between four contiguous planes. The other comparable combinations (three contiguous planes—AND—two contiguous planes anywhere, etc.) are tighter. The minimum penetration of our trigger is 4 cm iron and the rate is ~ 10 events per hour.

The gas mixture used under the Mont Blanc for streamer operation is one volume of argon, two volumes of CO_2, and one volume of N-pentane.

3. – Depth calculations.

The actual rock thickness along the different directions defined by the polar angle θ and ϕ have been derived from a detailed map of the mountain zone which gives isobases in 10 m interval. The presence of many peaks, as well as that of the glacier, has been taken into account. A sufficient density of points has been considered, so that by linear interpolation we can associate

---

([9]) G. Battistoni, E. Iarocci, M. M. Massai, G. Nicoletti and L. Trasatti: *Nucl. Instrum. Methods*, **164**, 57 (1979).

([10]) G. Battistoni, P. Campana, V. Chiarella, U. Denni, E. Iarocci and G. Nicoletti: *Nucl. Instrum. Methods*, **202**, 459 (1982).

to any directions (θ, ϕ) the relative slant depth with an accuracy better than 1 %, up to zenith angles of 65°. The data on the nature of the Mont Blanc rock come from two sets of measurements and give the following values: $A = 20.94$, $Z = 10.34$, $Z/A = 5.12$, $Z^2/A = 0.494$, $\varrho = 2.68$ g/cm^3. The conversion from the Mt. Blanc rock to standard rock is done using the results of Wright [11].

4. – Event selection and recording.

19416 muon events were recorded in the zenith angle $(0 \div 60)°$ during an effective working time of $6.4076 \cdot 10^7$ s from June 1982 to July 1984. In these events a general requirement is that the particles cross at least a thickness 27 cm in the apparatus in order to be classified as a muon. With this cut we obtain a well-defined geometrical acceptance within which the detection efficiency is practically 100 %. In order to check the muon parallelism in events with multiplicity $n \geqslant 2$, the angles between the tracks of the same event have been measured. In the sample with 2 muons (191 events) we find two events with tracks converging some metres above the apparatus. At this intersection point the distance between the tracks is 2.3 and 3.7 cm, while the relative angle between them is 16.1 and 1.5 degrees and as a consequence these events have been rejected. The distribution of the angle between the two tracks for the remaining 189 double muon events is displayed in fig. 1 and found in good

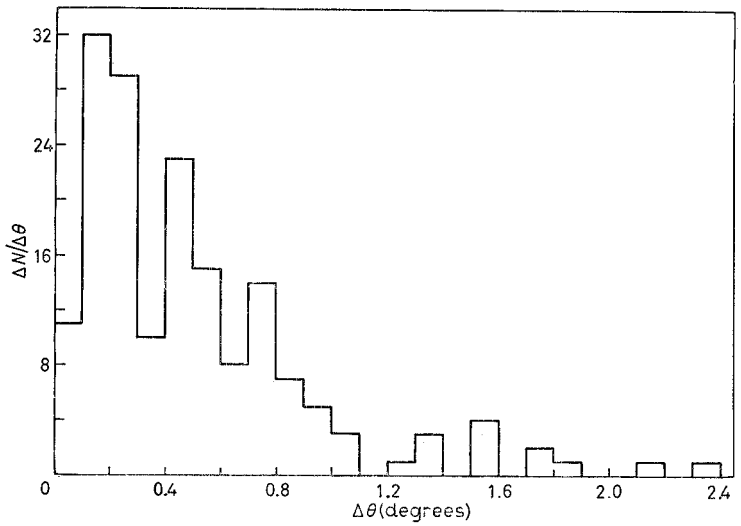

Fig. 1. – Distribution of the angle between tracks of muon pairs detected by NUSEX.

[11] A. G. WRIGHT: *Proceedings of the XIII International Cosmic Ray Conference* Vol. 3 (Denver, 1973), p. 1709.

agreement with the expectation from multiple Coulomb scattering in the rock and geomagnetic deflection (a minor contribution). The number of events of different multiplicities is reported in table I.

In fig. 2 an event with 5 parallel muons is shown.

TABLE I. – *Rate of multiple muons.*

Multiplicity n	Number of events	Time
1	19199	
2	189	
3	23	17854.4 hours
4	2	
5	2	
6	1	

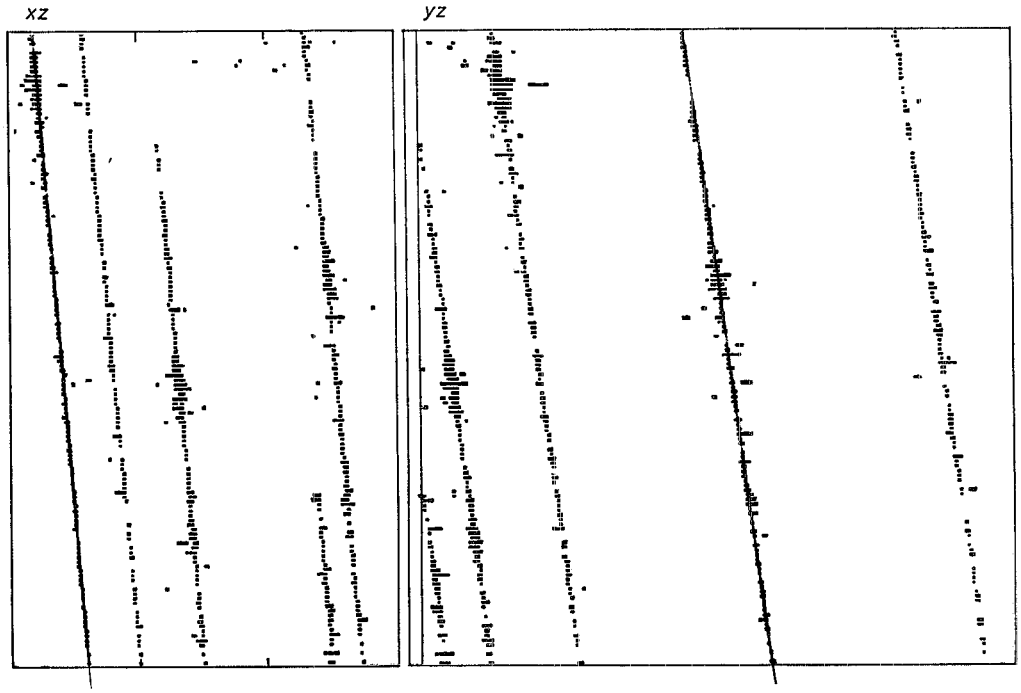

Fig. 2. – One event of five parallel muons seen in the two orthogonal views.

5. – Rate calculation.

The rates ϕ_n of events with exactly n muons in the detector can be calculated following the procedure described in [6].

The primary spectrum dN/dE_0 is described as a superposition of single

power spectra

$$\frac{\mathrm{d}N}{\mathrm{d}E_0} = \sum_i K_i(A) \cdot E_0^{-\gamma_i(A)} ,$$

where the summation is over all 5 groups of nuclei present in the primary flux (p, He, CNO, Mg, Fe). Here A is the average atomic number, $\gamma_i(A)$ is the power law spectral index eventually changing above a critical energy or rigidity, and the constants $K_i(A)$ depend on the normalization energy in the energy range of the direct measurements. Thus the muon bundles rate is given by

$$\phi_n = \sum_i K_i(A) \int E_0^{-\gamma_i(A)} \cdot P_n(E_0, A)\, \mathrm{d}E_0 ,$$

where $P_n(E_0, A)$ is the probability to sample muons of a shower resulting from the interaction of a primary of energy E_0 and mass A. This probability is described in terms of the average number of muons present above the threshold energy and their lateral distribution. As a consequences, it depends on the rock overbunden distribution. The evaluation of $P_n(E_0, A)$ requires the exact definition of the geometry of the apparatus and acceptance criteria, because the useful area as seen by the muon shower depends on the muon arrival direction in a complicated way. Moreover, the radial density distribution is expected to fall off rapidly with distance r from the shower axis so that its variation over the acceptance area has to be taken into account.

In conclusion $P_n(E_0, A)$ depends only on the interaction properties of high-energy hadrons and on the experimental conditions. As a result the astrophysical and particles physics aspects enter in a well-defined and separate way in the description of muon bundle rate.

The general procedure to calculate $P_n(E_0, A)$ in an analytical way is reported in the appendix. Briefly, the calculation proceeds through the following steps and assumptions:

i) Using the energy depth relation the average number of muons, with energy higher than a given threshold E_μ, present at a given slant depth h, is given as a function of the primary energy E_0 and mass A, $\bar{N}_\mu(E_0, A; > E_\mu)$.

ii) The muon number distribution around $\bar{N}_\mu$ follows a Poisson distribution. This result is expected if multiple-muon events are produced by nearly independent meson decays in the hadronic cascade, and has been confirmed by Monte Carlo calculations to be a very good approximation.

iii) Let $\bar{N}_\mu$ be the number of muons present at the level of the detector and p the probability for each muon to hit the acceptance area of the detector. Then, if we assume no correlation between all muons belonging to the same shower, the probability of detecting exactly n of the N_μ muons follows a bino-

mial distribution given by

$$\binom{N_\mu}{n} p^n (1-p)^{N_\mu - n} .$$

iv) The probability p depends on the muon lateral distribution density which we assume to be described by the following exponential form:

$$\varrho(r) = \frac{2}{\pi \langle r \rangle^2} \exp\left[-2r/\langle r \rangle\right],$$

where r is the distance from the shower axis and $\langle r \rangle$ is the mean radius of the distribution. For a primary of given energy E_0 and mass A, $\langle r \rangle$ depends on the energy threshold E_μ.

Thus, once the interaction model is defined, the average muon number $\bar{N}_\mu (E_0, A; > E_\mu)$ and the mean radius $\langle r \rangle$ $(E_0, A; > E_\mu)$ can be obtained. This allows us to calculate $P_n(E_0, A)$. We use the results of Monte Carlo calculations firstly developed by ELBERT (7) and then adapted to our experimental site (atmospheric depth at Mt. Blanc level, 690 (g/cm)^2, laboratory altitude 1380 m above the sea-level) by GAISSER and STANEV (8). The interaction model used assumes a total inelastic cross-sections increasing with energy as well as radial scaling of the Feynman x and P_T distributions of the produced particle. The mean transverse momentum $\langle P_T \rangle$ increases by 0.04 GeV/c per decade of primary energy above 1 TeV. At 100 TeV the $\langle P_T \rangle$ for secondary charged pions is 0.42 GeV/c. The muons result from pion and kaon decays. The deflection in the Earth's magnetic field, multiple-Coulomb scattering and muon energy loss are taken into account in propagating muons through the atmosphere and the rock up to the detector level. The resulting energy and radial muon distributions can be written as follows:

(1) $$\bar{N}_\mu(E_0, A; > E_\mu) = A \cdot G(E_\mu, E) \cdot \sec\theta , \qquad E = E_0/A ,$$

where

$$G(E_\mu, E) = 0.0145 \cdot (E/E_\mu)^{0.757} \cdot (1 - E_\mu/E)^{5.25}$$

with

$$E_\mu(\mathrm{TeV}) = 0.53 \cdot \left[\exp\left[0.4 \cdot h\right] - 1\right], \qquad h = \text{slant depth in km w.e.},$$

(2) $$\langle r \rangle (E_0, A; > E_\mu) = A(E_\mu) + B(E_\mu) \cdot (E_\mu/E)^{0.62} \cdot \sec\theta$$

with

$$A(E_\mu) = 3.13 E_\mu^{-0.46}, \quad B(E_\mu) = 13.2 E_\mu^{-0.31} \qquad E_\mu \text{ in TeV}.$$

In writing (1) and (2) it is assumed: 1) a cascade produced by a nucleus of energy E_0 and mass A is equivalent to A nucleon cascades of energy E_0/A;

2) the lateral distribution depends only on the primary energy per nucleon and not on the muon multiplicity.

6. – Comparison with observation.

We have calculated the expected multiple-muon rates for four trial compositions recently adopted in interpreting various cosmic-ray phenomena:

i) The « constant-mass composition » quoted by KEMPA and WDOWCZYK ([5]) obtained by an extrapolation of the directly measured spectra with a single constant differential slope, $\gamma = 2.71$, up to a fixed magnetic rigidity $R_c = 2 \cdot 10^6$ GeV/c. Beyond this, the spectra steepen to $\gamma = 3.0$. The correspond breaks for groups of nuclei different from the proton are at total energy $= (A/2) \cdot R_c$.

ii) A low-energy composition (LEC) quoted in ([4a]) with differential spectral index of 2.71 for all species. Even this model refers to the low-energy primary composition measured directly at energies up to about 100 GeV/ /nucleon. We assume that the spectral index changes to 3.0 at a critical energy $2 \cdot 10^{15}$ eV.

iii) The « Fuji spectrum » derived by the Fuji group ([12]) in order to fit the observed rate of γ-ray families by means of an interaction model in which the scaling holds around 10^3 TeV. The spectral indices are 2.8, 2.8, 2.6, 2.6, 2.3 for the five groups. The absolute intensity of each component is normalized to those given by JULIUSSON at 1 TeV/nucleus ([13]). This model is strongly dominated by heavy primaries (68% iron and only 9% protons at 10^{15} eV). The fractions become constant above $2 \cdot 10^{15}$ eV and all components assume the same slope, $\gamma = 3.0$.

iv) The « Maryland spectrum » ([1e]) derived from measurements on time structure of hadrons near air shower cores. In this model the iron group has a spectral index of 2.39 making up about 65% of the primaries above $2 \cdot 10^{15}$ eV, while the other groups have an index of 2.68. The energy cut-off is taken at $2 \cdot 10^{15}$ eV above which all components steepen to a differential slope of 3.0.

The comparison between measured and calculated rates is shown in fig. 3.

An inspection of this figure shows that the constant mass composition gives the best agreement with our data. Even the predictions of the Maryland composition are reasonable, being only a factor two higher for double and triple

---

([12]) *a)* S. TORII: *Proceeding of the Workshop on Very High-Energy Cosmic Ray Interactions, University of Pennsylvania, Philadelphia, April 22-24, 1982*, edited by M. L. CHERRY, K. LANDE and R. I. STEINBERG; *b)* E. JULIUSSON: *Proceeding XIV International Cosmic Ray Conference*, Vol. **8** (München, 1975), p. 2689.

([13]) L. BERGAMASCO, H. BILOKON, A. CASTELLINA, B. D'ETTORRE PIAZZOLI, G. MANNOCCHI, P. PICCHI and S. VERNETTO: *Nuovo Cimento C*, **6**, 569 (1983).

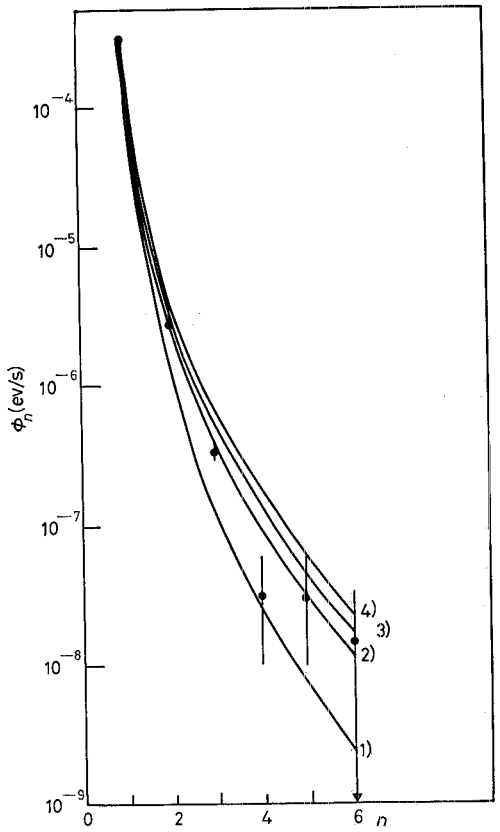

Fig. 3. – Comparison between experimental rates and predictions from four trial models for the primary spectrum and composition. 1) LEC, 2) constant mass composition, 3) Maryland spectrum, 4) Fuji spectrum.

muons. We stress that this agreement was obtained without any normalization procedure. LEC and Fuji spectra fail in explaining the data, the former because of the nonadequate normalization, the latter because it is too rich in heavy nuclei.

The rates calculated by means of the constant mass composition are about (10÷15)% higher than the experimental ones in the range of significant statistics ($n = 1 \div 3$). Since the contribution to these multiplicities comes essentially from light nuclei, a suitable adjustment of the shape of proton and helium spectra could restore a better agreement. On the other hand, recent direct measurements by the JACEE collaboration ([14]) give a steeper spectral

([14]) T. M. BURNETT, S. DAKE, M. FUKI, J. C. GREGORY, T. HAYASHI, R. HOLYNSKI, R. W. HUGGETT, S. D. HUNTER, J. IWAI, W. V. JONES, A. JURAK, J. J. LORD, O. MIYAMURA, T. TOMINAGA, J. W. WATTS, B. WILCZYNSKA, R. J. WILKES, W. WOLTER and B. WOSIEK: *Phys. Rev. Lett.*, **51**, 1010 (1983).

index for protons and helium nuclei at energies above a few TeV/nucleon. Also the all nucleon flux previously obtained at Mt. Blanc ([13]) suggests a spectral index between 2.75 and 2.8. Moreover, a preliminary analysis of NUSEX data gives a muon differential energy spectrum consistent with a primary all-nucleon flux following a dependence $E^{-2.77}$ in the range $(10^{13} \div 2 \cdot 10^{14})$ eV.

Guided by these considerations we assumed a value of -2.75 for the spectra index of protons and helium nuclei. We normalized the flux at 10 TeV to the JACEE data (in agreement with other direct measurements) and treated the iron spectral index as a free parameter. The iron is normalized to a flux of $2.42 \cdot 10^{-5}$ particles/(m^2·sr·s·GeV/nucleon) at 100 GeV/nucleon, consistent with balloon observations. This procedure restores the agreement between experimental and calculated rates at the lowest multiplicities ($n = 1, 2$) which are determined essentially by protons and helium nuclei, whereas predicted rates at higher multiplicities show an increasing dependence on iron percentage.

The results are shown in fig. 4. For multiplicities $\geqslant 4$ the calculated rates

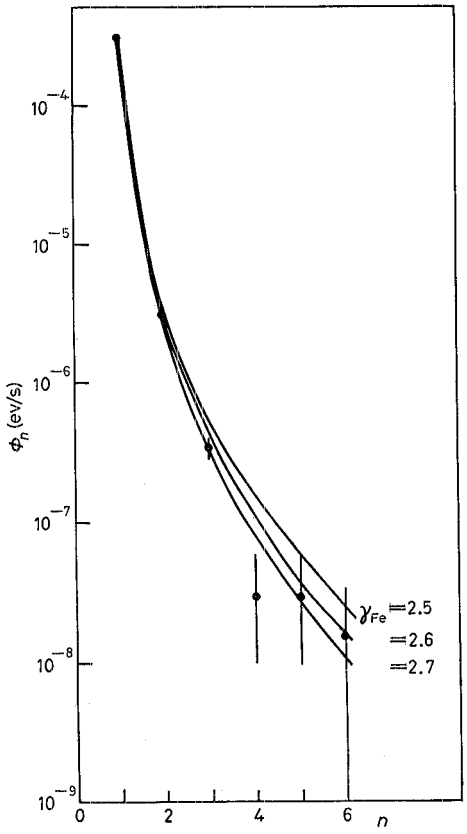

Fig. 4. – Comparison between experimental rates and the predictions of our model of the primary composition (see text) for different values of the iron group spectral index.

for $\gamma_{Fe} = 2.5$ are about a factor of 2 larger than the ones calculated with $\gamma_{Fe} = 2.7$. It is clear that, in spite of the statistical uncertainties of the data for $n \geqslant 4$, the predicted rates could agree with the experimental ones only if we assume a spectral index for the iron group higher than 2.5. The overall best agreement is found for iron spectral index in the range $2.6 \div 2.7$.

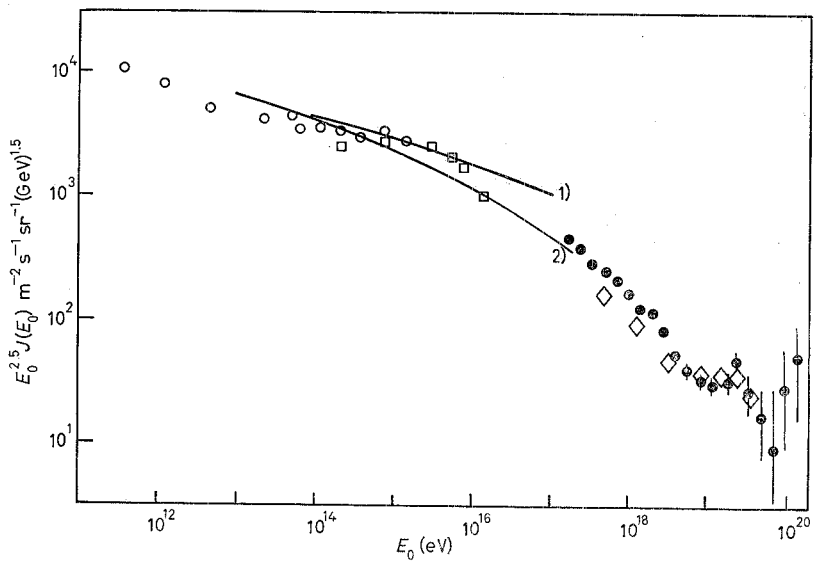

Fig. 5. – Comparison between predictions of our model with $\gamma_{Fe} = 2.5$ (curve 1)) and 2.7 (curve 2)) and the all particle flux J (E_0). E_0 is the energy per nucleus. The experimental points come from measurements of the flux by balloons, γ-ray families and air shower size as summarized in ref. ([15]).

This model reproduces very nicely both the all-nucleon flux measured at Mt. Blanc ([14]) in the range $(10^{13} \div 10^{14})$ eV and the all-particle flux between 10^{13} and 10^{16} eV. In fig. 5 the all-particle flux predicted by our model is compared with the all-particle flux measured by the Proton Satellite experiments or determined from measurements of air shower size. The data compilation is from ([15]).

In fig. 6 the differential rates for each primary component are shown to put in evidence the increasing contribution of heavy nuclei and the shift towards higher energies with multiplicity. Single muons are due essentially to interactions of primary protons and helium nuclei ($\sim 90\%$) at energies around 10^{13} eV, the contribution of Mg and Fe groups being only about 5%. The relative

([15]) A. M. HILLAS: *Proceedings of the Cosmic Ray Workshop*, edited by T. K. GAISSER (Newark, 1983), p. 16.

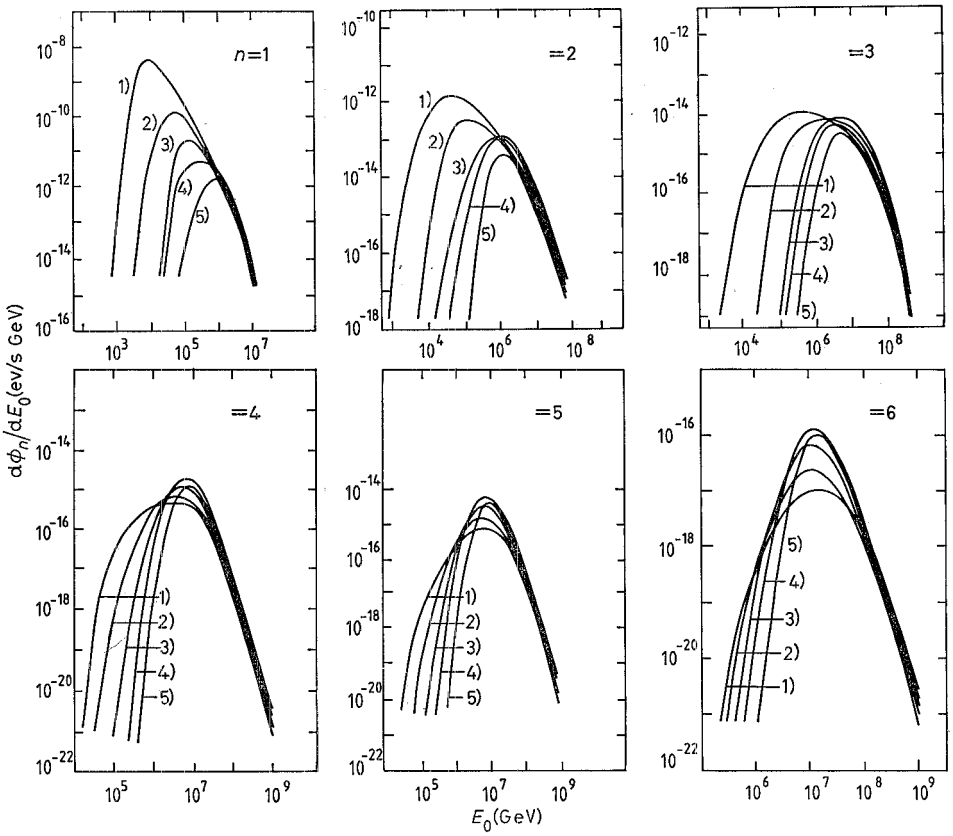

Fig. 6. – The rate of muon bundles of multiplicity n as a function of the energy E_0 and mass A of the primary cosmic rays. The numbers attached to the curves identify the five mass groups p, He, CNO, Mg, Fe. The calculations refer to our model of the primary composition with $\gamma_{Fe} = 2.7$.

weight to events of high multiplicity, $n = 5$, 6, changes to 15% and 66% respectively, the main contribution coming from primaries with energies around 10^{16} eV.

Normalization coefficients, slopes and breaking points for all components are summarized in table II.

TABLE II. – *Normalization coefficients, spectral index and points of change of slope.*

	K_1	γ_1	E_c (GeV)
p	$2.27 \cdot 10^4$	2.75	$2 \cdot 10^6$
He	$1.21 \cdot 10^4$	2.75	$4 \cdot 10^6$
CNO	$6.20 \cdot 10^3$	2.71	$1.4 \cdot 10^7$
Mg	$9.20 \cdot 10^3$	2.71	$2.6 \cdot 10^7$
Fe		$2.6 \div 2.7$	$5.2 \cdot 10^7$

The iron group is normalized to a flux of $2.42 \cdot 10^{-5}$ particles/(m^2·sr·s··GeV/nucleon) at 100 GeV/nucleon.

The spectrum is represented by $K_1 \cdot E_0^{-\gamma_1}$ for $E_0 < E_c$ [E_0, GeV] and $K_2 \cdot E_0^{-3.0}$ for $E_0 > E_c$. The units of K are $(\mathrm{m}^{-2}\,\mathrm{s}^{-1}\,\mathrm{sr}^{-1}\,(\mathrm{GeV})^{-1})$.

7. – Discussion and conclusions.

We have determined a primary cosmic-ray spectrum by requiring the agreement between the measured and calculated rates of multiple-muon events. A successful understanding of the observations requires an energy spectrum for heavier nuclei not very far from the spectra of the other nuclear groups. Though the obtained agreement between observations and predictions is excellent, it should be emphasized that many assumptions are required to define the spectra of different nuclear groups and the critical energies above which these spectra steepen. The choice of the normalization points is somewhat arbitrary for nuclei other than protons and helium, and the extrapolation to high energy of the light and medium-heavy nuclei spectra is mainly suggested by theoretical considerations. The choice of a spectral index of 2.71 for CNO and Mg groups agrees with the requirements of the leaky box model, but low-energy data are somewhat flatter. We have checked these possibilities by considering a flatter behaviour of the CNO group and different values for the critical energy or rigidity. The spectra which we obtain are the result of a compromise between a fair agreement with muon rates and the need to reproduce the all particle spectrum. In any case the iron spectrum index cannot be lower than 2.5.

Another source of uncertainty is the description of the hadronic interaction at very high energy. In order to predict the rates of multiple muons we used results of Monte Carlo calculations which extrapolate to very high energy the information from accelerator measurements. Although measurements by CERN $\mathrm{p\bar{p}}$ collider experiments show that scaling violations are small at laboratory energies $\sim 1.5 \cdot 10^{14}$ eV, many phenomena in cosmic-ray physics (like Centauro events) have suggested 100 TeV/nucleon to be a threshold for a change in properties of the hadronic interaction. Theoretical speculations about nucleus interaction foresee the possibility of the transition to a quark-gluon phase at these energies. An increased yield of muons should be expected ([16]). The flux of high-multiplicity muon events in the NUSEX experiment seems not to support these ideas.

Summarizing, we used 1) an interaction model based on Feynman scaling, energy-dependent total cross-sections and inclusive distributions from accelerator data, 2) a primary composition with an iron spectrum only slightly

([16]) R. Anishety, P. Koehler and L. McLerran: *Phys. Rev. D*, **22**, 2793 (1980).

flatter than the proton one. This successfully reproduces the NUSEX muon bundle rates. Our data do not exhibit any appreciable deviation from this picture in the limit of statistical significance.

* * *

We acknowledge the kind collaboration of T. K. GAISSER and T. STANEV, who sent us their results of Monte Carlo calculations tuned to the Mt. Blanc environment.

We also express our gratitude to our technical staff, for their friendly support during every phase of the experiment, and to the Management of « The Società Italiana del Monte Bianco » for their kind collaboration.

APPENDIX

Calculation of the probability $P_n(E_0, A)$.

By using the assumptions and definition of sect. **5** the probability $P_n(E_0, A)$ can be calculated as follows (ref. (6)):

$$P_n(E_0, A) = \int_0^{\infty} \cos\theta \, R \, \mathrm{d}R \int_0^{2\pi} \frac{\mathrm{d}P_n}{\mathrm{d}\sigma}(E_0, A)\, \mathrm{d}\phi$$

with

$$\frac{\mathrm{d}P_n}{\mathrm{d}\sigma}(E_0, A) = \int_0^{2\pi} \mathrm{d}\varphi \int_0^{\theta_M(\varphi)} \frac{\mathrm{d}P_n}{\mathrm{d}\sigma\, \mathrm{d}\omega}(E_0, A) \sin\theta \, \mathrm{d}\theta \, .$$

$\mathrm{d}P_n(E_0 A)/\mathrm{d}\omega \, \mathrm{d}\sigma$ is the probability of sampling n muons produced by a primary of mass A and energy E_0. $\omega(\theta, \varphi)$ is the arrival direction of the showers whose axis hits the horizontal plane in a point having polar co-ordinates (R, ϕ) inside the elements of area $\mathrm{d}\sigma = \cos\theta \, R \, \mathrm{d}R \, \mathrm{d}\phi$. In our analysis we cut at zenith angle at $\theta = 60°$ so that $\theta_M(\varphi)$ does not depend on azimuthal angle.

The differential probability is given by

$$\frac{\mathrm{d}P_n}{\mathrm{d}\sigma\, \mathrm{d}\omega}(E_0, A) = \sum_{N_\mu \geqslant n} P_{\bar{N}_\mu}(N_\mu) \frac{\mathrm{d}p_n}{\mathrm{d}\sigma\, \mathrm{d}\omega}(E_0, A) \, ,$$

where

$$P_{\bar{N}_\mu}(N_\mu) = \frac{\exp[-\bar{N}_\mu] \cdot \bar{N}_\mu^{N_\mu}}{N_\mu !}$$

is the probability of finding N_μ muons, $\bar{N}_\mu(E_0, A; > E_\mu)$ being the muon average number. $\mathrm{d}p_n/\mathrm{d}\omega \, \mathrm{d}\sigma(E_0, A)$ is the probability of detecting exactly n of the N_μ

incident muons. For this we have

$$\frac{\mathrm{d}p_n}{\mathrm{d}\sigma\,\mathrm{d}\omega}(E_0, A) = \binom{N_\mu}{n} \cdot [\varrho S]^n \cdot (1 - [\varrho S])^{N_\mu - n},$$

where

$$[\varrho S] = \cos\theta \cdot \int_{x_m}^{x_M} \int_{y_m}^{y_M} \varrho(r)\,\mathrm{d}x\,\mathrm{d}y$$

is the probability for each muon to hit the acceptance area. Here $\varrho(r)$ is the lateral distribution density normalized to one, and r is the distance from the shower axis measured in a plane orthogonal to it:

$$r(R, \phi; \theta, \varphi; x, y) = \{(R\cos\phi - x)^2 + (R\sin\phi - y)^2 - \\ - [\sin\theta\cos\varphi \cdot (R\cos\phi - x) + \sin\theta\sin\varphi \cdot (R\sin\phi - y)]^2\}^{\frac{1}{2}}.$$

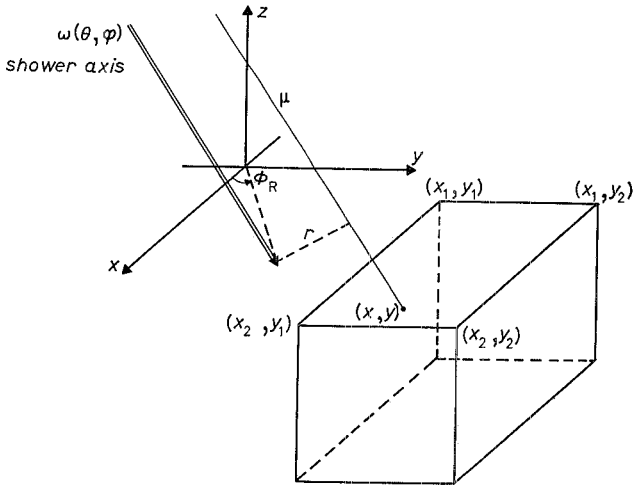

Fig. 7. – Co-ordinates and geometric parameters used in the text.

The integration is performed within limits defined by experimental conditions. If x_1, x_2, y_1, y_2 are the co-ordinates of the edges of the detector —see fig. 7—and z_1 is the minimum detector thickness that the muon must cross in order to be detected and accepted, we get

$$x_m = x_1 + f_m \cdot \mathrm{tg}\theta\cos\varphi,$$
$$x_M = x_2 + f_M \cdot \mathrm{tg}\theta\cos\varphi,$$
$$y_m = y_1 + g_m \cdot \mathrm{tg}\theta\sin\varphi,$$
$$y_M = y_2 + g_M \cdot \mathrm{tg}\theta\sin\varphi,$$

where f_m, f_M, g_m, g_M are defined in table III.

TABLE III.

φ	$0 \div \pi/2$	$\pi/2 \div \pi$	$\pi \div (3/2)\pi$	$(3/2)\pi \div 2\pi$
f_m	z_1	$z - z_1$	$z - z_1$	z_1
f_M	$z - z_1$	z_1	z_1	$z - z_1$
g_m	z_1	z_1	$z - z_1$	$z - z_1$
g_M	$z - z_1$	$z - z_1$	z_1	z_1

Here z is the height of the module.

Since the detector operates underground the slant depth, and so the energy threshold E_μ, depend on the direction $\omega(\theta, \varphi)$. In other words we have $E_\mu = E_\mu(h[\theta, \varphi])$, thus the neam $\bar{N}_\mu(E_0, A; > E_\mu)$ and the lateral distribution density $\varrho(r)$—through the mean radius $\langle r \rangle$—depend on the direction. A detailed map of the surrounding mountains allows us to know with good precision the effective energy threshold corresponding to any direction and calculate accordingly the mean number and radius of the muon distribution.

● RIASSUNTO

Le frequenze di muoni multipli ottenute con il rivelatore NUSEX ad una profondità verticale di 5000 hg/cm^2 sono confrontate con diversi modelli sulla composizione di primari cosmici. Questo studio è fatto usando Montecarlo e formule analitiche che tengono conto degli aspetti geometrici e dell'accettanza dell'apparato. Un buon accordo è trovato con un modello nel quale la relativa frazione di nuclei pesanti non cresce significatamente fino a 10^{16} eV. Questo modello riproduce bene sia il flusso totale di nuclei misurato nell'intervallo $(10^{13} \div 10^{14})$ eV che lo spettro di particelle fino a 10^{16} eV.

Спектр первичных космических лучей при энергиях $(10^{13} \div 10^{16})$ эВ из множественных мюонных событий в NUSEX эксперименте.

Резюме (*). — Интенсивности множественных мюонных событий, измеренных в NUSEX эксперименте на глубине 5000 hg/cm^2 s.r., сравниваются с имеющимися моделями первичного состава космических лучей. При вычислениях используются моделирования по методу Монте-Карло и аналитические формулы, которые учитывают геометрические характеристики аппаратуры. Получается хорошее согласие с моделью, в которой относительная доля первичных тяжелых ядер существенно не увеличивается вплоть до энергий 10^{16} эВ. Эта модель очень хорошо воспроизводит поток всех нуклонов, измеренных в области $(10^{13} \div 10^{14})$ эВ, и спектр всех частиц вплоть до 10^{16} эВ.

(*) *Переведено редакцией.*